Title
OPTICAL SYSTEMS FOR SYNCHROTRON RADIATION: LECTURE 4. SOFT X-RAY IMAGING SYSTEMS

Author
Howells, M.R.

Publication Date
1986-04-01

Lawrence Berkeley Laboratory
UNIVERSITY OF CALIFORNIA

Accelerator & Fusion Research Division

Presented at the Scottish Universities Summer School in Physics on Synchrotron Radiation Sources and Their Applications, Aberdeen, Scotland, September 14-28, 1985

OPTICAL SYSTEMS FOR SYNCHROTRON RADIATION:
LECTURE 4. Soft X-Ray Imaging Systems

M.R. Howells

April 1986

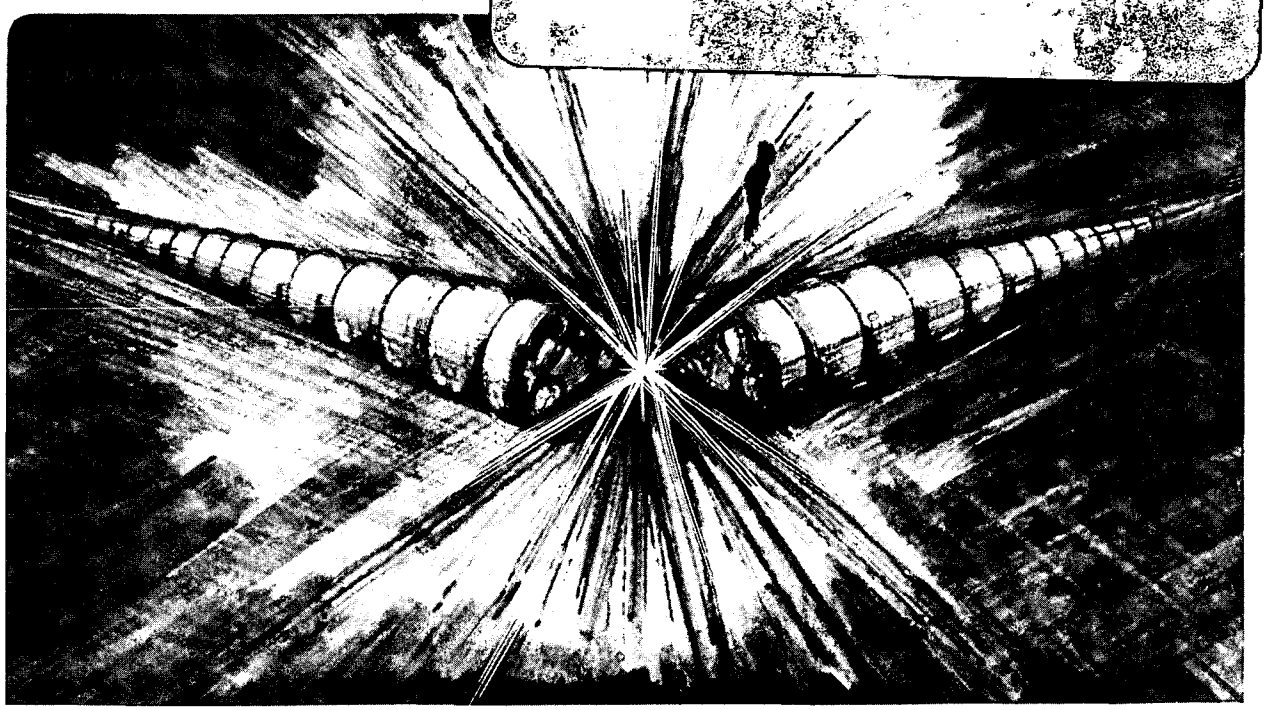

Prepared for the U.S. Department of Energy under Contract DE-AC03-76SF00098

DISCLAIMER

LBL-21365

OPTICAL SYSTEMS FOR SYNCHROTRON RADIATION:
Lecture 4. Soft X-ray Imaging Systems

M.R. Howells

Center for X-ray Optics, Lawrence Berkeley Laboratory
University of California
Berkeley, California 94720

April 1986

This work was supported by the Office of Basic Energy Sciences,
U.S. Department of Energy, under Contract # DE-AC03-76SF00098.

LBL 21365

OPTICAL SYSTEMS FOR SYNCHROTRON RADIATION
(A Series of Four Lectures)
LECTURE 4:
SOFT X-RAY IMAGING SYSTEMS

M. R. Howells
Center for X-ray Optics, Lawrence Berkeley Laboratory,
University of California
Berkeley, California 94720

1. INTRODUCTION

x-ray imaging in its widest sense includes a vast range of subjects from tomography to crystallography and from auto radiography to conventional clinical shadow-casting. In this article we deal with the restricted class of imaging experiments where soft x-rays are used to study biological material at the cellular or sub-cellular level. In other words we are discussing microscopes that use soft x-rays. We briefly review the history of this type of measurement and consider the special features of high brightness synchrotron radiation sources which make them particularly suited to soft x-ray imaging. We deal with the five most popular technical approaches to imaging biological material with soft x-rays and give a comparison of their characteristics.

There is a considerable literature associated with this field. Three conferences[1-3] have been dedicated to it and several recent reviews[4-6] exist. There are also reviews and conference proceedings from the pre 1970 period that contain sections on x-ray imaging.[12] The book by Cosslett and Nixon[7] provides an excellent treatment of the background against which modern developments have been taking place.

This work was supported by the Office of Basic Energy Sciences,
U.S. Department of Energy, under Contract # DE-AC03-76SF00098.

2. HISTORY

The first successful attempts to form x-ray images took place in the last years of the nineteenth century. A photographic plate was exposed to x-rays through a sample that was in contact with the plate[8]. The plate was then developed and the resulting pattern, known as a "contact microradiograph" was examined under the light microscope.

To achieve resolution superior to that of the light microscope was apparently possible in principle but without a source of submicron dimensions or a higher resolution detector or an optical system that could provide magnification, development of the x-ray microscope remained blocked for several decades. The first successful x-ray "lens" was reported by Kirkpatrick and Baez[9] in 1948 and marked the beginning of a long struggle, which still continues today, to solve the technical problems involved in producing a high resolution x-ray microscope objective. The Kirkpatrick-Baez scheme involved two spherical reflectors working at extreme grazing incidence and arranged so that the plane of incidence of the second was perpendicular to that of the first. In this way, each mirror provided focussing in one plane and, to first order, did nothing in the other. This method was successful in making magnified x-ray images but was prevented by aberrations and surface finish considerations from achieving resolution superior to the light microscope. Subsequently more sophisticated reflection systems[10] have been tried but in spite of the application of improved manufacturing methods they have all been overtaken in resolution by the Fresnel Zone Plate x-ray lens to which we return later. A different approach which was developed in the 1950's was the so-called "Projection Microscope"[7]. In this instrument an electron microscope type focussing system was used to produce a small focal spot on an x-ray anode. This "microfocus" source was placed in front of the sample and a photographic plate was located at a considerable distance behind the sample. The plate recorded a magnified projection of the sample, limited in resolution mainly by diffraction. This system reached the point of commercial production[11] but again did not improve on the resolution of the light microscope.

A number of technical developments have occurred in the last 15 years

which bear on soft x-ray imaging and give reason to hope that we are just beginning a period of rapid development in this old field. These are (i) the development of high spectral brilliance synchrotron radiation sources, especially undulators, (ii) the development of microfabrication methods for microcircuits, particularly electron beam writing, (iii) the availability of high resolution x-ray resists and (iv) the demonstration of high resolution holographic methods for producing diffractive optics. All these are being used and are discussed below. The technical development that has not yet occurred but which is approaching is the 1μm resolution, photon counting, area detector. This will make a great impact on the field if and when it comes.

3. PRESENT TECHNIQUES

Because of the relative speed with which these technologies have become available there has been very little shake-out in the field and researchers are still largely following their hunches. This leads to a wide variety of approaches being studied simultaneously. We have choosen five methods for consideration here.

(i) Contact microscopy

(ii) Zone plate imaging

(iii) Scanned image zone plate microscopy

(iv) Scanned image reflection microscopy

(v) Holography and diffraction

In this article we give brief descriptions of these methods in sections 7-11 together with references and status reports.

4. SCIENTIFIC MOTIVATION FOR X-RAY IMAGING

The main reason for interest in soft x-ray imaging is that it holds the promise of filling in certain gaps in the capability offered by the present successful methods for imaging biological material. These are electron microscopy, visible light microscopy and x-ray crystallography. Visible light microscopy is in many respects the most universal tool but is limited in resolution by the wavelength of light. Both the other methods give superbly good resolution but require the sample to be in non-biological form i.e. crystalline for crystallography or cut into thin sections, dehydrated and stained with heavy metals for many electron

microscopy applications. These requirements originate from the atomic interaction cross-section of the particles[6,13] used in crystallography and electron microscopy. Hard X-rays (~1Å wavelength) have a cross section which is lower than one would like so that its weak interaction with the sample must be magnified by assembling millions of samples (the crystal) and superposing their signals. The atomic cross section of the electrons used in microscopy (generally 10-100 keV energy) is too large and has insufficient difference (contrast) among the interesting sample materials and water. Hence, the need for sectioning (thinning) and staining. On the other hand, soft x-ray photons around 30Å have about the right penetration for imaging an intact, wet cell and, moreover, have a natural contrast mechanism enabling them to "see" carbon and nitrogen containing materials "through" a background of water. Consider the data plotted in figure 1.[13] The difficulties with electrons, poor penetration and lack of contrast between biological material and water, are very evident. In addition it is apparent that for soft x-rays there exists a privileged region of the spectrum between the O_K and C_K absorption edges where carbon containing materials absorb and can be imaged and water is relatively transparent. This region is known as the "water window" and allows in principle, at least, the use of x-ray edges to give elemental contrast in absorption imaging.[14] The use of edges in this way is not limited to mapping carbon and nitrogen but can be applied quite generally. There are, of course, various limitations that we have not mentioned but the main points are that by using x-ray edges one can obtain greatly improved detectability thresholds in microanalysis and a much larger information to damage ratio in microscopy.[15]

5. THE PHYSICS OF X-RAY IMAGING

All methods of x-ray imaging involve illuminating the sample with x-rays and utilization of the resulting wave field (transmitted plus scattered) to get information about the sample. Therefore we need a suitable physical description of the interaction of the x-ray beam with the sample. Suppose we represent the electric field vector of the x-ray beam by $\psi(\underline{r})$. We know that in general ψ must satisfy the Helmholtz equation.

$$\nabla^2\psi + k^2\psi = 0 \qquad (1)$$

where $k = 2\pi/\lambda$ and we have suppressed the time dependance. We can rewrite this in terms of k_o the free space value of k and the refractive index of the medium n by noting that $k=k_o n$ and so

$$\nabla^2\psi + k_o^2\psi = (1-n^2)k_o^2\psi \equiv U\psi \qquad (2)$$

where it is understood that n is a function of space and represents the sample. The solution of this equation[16] can be written as an integral equation (see figure 2 for the notation) as follows:

$$\psi(\underline{r}) = e^{ik_o z} - \frac{1}{4\pi}\int_{\text{sample}} \frac{\exp ik_o|\underline{r}-\underline{r}'|}{|\underline{r}-\underline{r}'|} U(\underline{r}')\psi(\underline{r}')d^3\underline{r}'. \qquad (3)$$

In words, each element $d^3\underline{r}'$ of the sample depletes the incoming beam by scattering a secondary wavelet of strength $-\frac{1}{4\pi}U(\underline{r}')$ times the amplitude incident on the element. For the three dimensional scattering objects which are of interest in soft x-ray imaging experiments we think of the object as a complex refractive index distribution $n(\underline{r})$ where the local index is a weighted average of that due to the various atomic constituents, i.e.

$$n(\underline{r}) = 1 - \sum_j \frac{2\pi N_j(\underline{r})r_o^2}{k_o^2}(f_{1j}+if_{2j}) \qquad (4)$$

where r_o is the classical electron radius and $N_j(\underline{r})$ is the local number density of atoms of type j with scattering factor $f_j=f_{1j}+if_{2j}$.[13]

The techniques for soft x-ray imaging depend on measurement of the scattered field and the use of various strategies to solve the inverse scattering problem and produce a useful reconstruction of $n(\underline{r})$. Sometimes this is done by analogue methods. Sometimes digital ones are needed. We return to this subject later.

The atomic cross-section for photoelectric absorption σ_a is given by (see lecture 1 of this series)[13]

$$\sigma_a = 2r_o\lambda f_2 \qquad (5)$$

whilst the cross section for coherent (Thomson) scattering is given by $8\pi r_o^2/3$ per electron. In the soft x-ray part of the spectrum photon wavelengths are much greater than atomic sizes. Therefore the cross-section (σ_s) for a whole atom containing effectively $f=f_1+if_2$ electrons

arises from coherent superposition of the scattering amptitudes of the individual electrons. σ_s is thus given by $|f|^2$ times the Thomson cross-section.

$$\sigma_s = \frac{8\pi r_o^2}{3} \quad (f_1^2+f_2^2) \qquad (6)$$

It should be noted that although the photoelectric cross-section is usually about 10^4 times larger than the coherent cross-section,[17] this does not mean that it dominates the imaging process. Indeed, it is clear from (5) that the existence of phase change effects (described by f_1) and absorption (described by f_2) BOTH lead to scattering.[24] The roles of these two effects in producing scattering are well illustrated by the known types of transmission diffraction gratings (or zone plates). Some depend purely on absorption (amplitude gratings). Others on phase effects (phase gratings). It is known that phase gratings are more efficient performers[(18)] but not by a large margin.

6. SOURCES

The requirements for a source for soft x-ray imaging experiments have been discussed by the group working at Brookhaven's National Synchrotron Light Source[(19)] and in studies stimulated by plans for the "Advanced Light Source" at Lawrence Berkeley Laboratory.[(20)] The main questions concern the degree of coherence required. The physics of the coherence properties of electromagnetic fields have been treated in a number of excellent texts[(21,22)] and articles[(23)] and are usually divided into questions of temperal and spatial coherence.

The temperal coherence of a beam of light is usually described by a coherence "length" (ℓ_c) which is roughly the length of the electromagnetic wave train and is connected to the monochromaticity $\lambda/\Delta\lambda \equiv N$ by the relation

$$\ell_c = \frac{\lambda^2}{\Delta\lambda} \equiv N\lambda \qquad (6)$$

ℓ_c is the path difference that can be tolerated between two interfering beams (derived from the original one by amplitude division, say) for a given loss of fringe contrast.

The spatial coherence of a beam of light is described by a transverse area (the "coherence patch") within which pieces of wavefront could be

split (by wavefront division) and recombined to form fringes of at least a given contrast. The angular subtense of the patch is given roughly by λ/s where s is the source width. If the source emits only into the coherence patch it is said to be fully spatially coherent or "single mode". From the above, a single mode beam of light such as that from a well prepared laser has an emittance $\varepsilon \sim \lambda$ so that the phase space volume of a spatially coherent beam of light (including both transverse dimensions) is of order λ^2. For λ=30Å, for example

$\varepsilon_{30Å} \sim 30Å.\text{radians} \equiv 3\times10^{-3}$ mm.mradian

For a synchrotron radiation source we usually characterise its strength by a spectral brilliance (B) expressed as

B = ? photons/sec/mm^2/mradian^2/0.1% bandwidth.

i.e. B is the flux per unit bandwidth per unit phase space volume (see fig 11). The part of B that is spatially coherent is that part in a phase space volume λ^2 so we see that the coherent flux per unit bandwidth is $B\lambda^2$. This shows that for imaging methods needing a coherent illuminating beam the spectral brilliance B is the figure of merit of the source. If we insist on a certain fixed coherence length then from (7) the bandwidth is $\frac{\lambda}{\ell_c}$ and the coherent flux is $B\lambda^3/\ell_c$ demonstrating the extreme difficulty of coherence experiments at very short wavelengths.

7. CONTACT X-RAY MICROSCOPY

This is, so far, the most successful x-ray microscopy and the only one which is at all widely used in the biological community.[25] It is really the modern counterpart of the early method called x-ray microradiography which used photographic film as a detector. The present day method has been developed at the IBM Watson Laboratory by R. Feder and D. Sayre. It achieves high spatial resolution (50-100Å at best) by the use of a high resolution x-ray resist such as polymethyl methacrylate (PMMA).[26] The resist is exposed to the x-ray beam through the sample and thus gives a shadow picture limited in spatial resolution by the intrinsic resolution of the resist and by diffraction. The latter is roughly given by $\sqrt{\lambda t}$, where t is the sample feature to resist distance. Diffraction is

significant for sample thicknesses greater than about 250Å, which includes most cases. After exposure the resist is developed, typically in methyl iso-butyl ketone, and examined in the scanning electron microscope for qualitative results or better in the transmission or scanning transmission electron microscope for more quantitative work. For a practical description see reference 4. For a typical picture see fig 3.

Contact microscopy is very undemanding on the temporal and spatial properties of the illuminating beam and thus it can be implemented with a simple source such as an x-ray tube or with a single pulse of a pulsed source. The latter method can be effective in freezing the motion of an initially living sample and can also mitigate the effects of radiation damage if the pulse is fast enough (picoseconds or less).[27] Without a pico-second pulse the sample damage involved in this technique is considerable unless the sample is more radiation resistant than PMMA which is usually not the case.

8. ZONE PLATE IMAGING

This method requires little description because of its similarity in principle to the visible light microscope. The optical system[28] begins (figure 4) with a large condenser zone plate which images at less than diffraction limited resolving power and condenses the beam on to a pinhole. Since the focal length of a zone plate varies like $1/\lambda$, the zone plate-plus-pinhole amounts to a monochromator as well as a condenser. The sample is placed in or near the pinhole and is illuminated with the more or less spatially incoherent beam. Each piece of the sample then becomes a source of secondary scattered wavelets which is imaged by a small "micro zone plate". The latter gives a diffraction limited image with sufficient magnification to allow the use of a low resolution detector such as film or an electronic device.

This scheme is only apparently simple because to get high resolution one has to make a zone plate whose narrowest zone spacing is equal to the desired diffraction limited image resolution. Most of the successes with this technique have been achieved by the Gottingen group who have perfected a highly specialised ultra-violet (UV) holographic technique for making zone plates with the capability for achieving diffraction limited

resolution in the x-ray region. The method[29] involves using deliberately aberrated waves to record the hologram (zone plate) so that the spherical aberration (which would otherwise be inherent in using a UV recorded zone plate at x-ray wavelengths) is cancelled. An object space resolution of 550Å has been demonstrated using this method.

The main advantage of the technique is its use of an essentially spatially incoherent illuminating beam. This, together with the fact of imaging all sample pixels simultaneously leads to very fast picture taking - a few seconds, at present, using a BESSY bending magnet source. On the other hand, the micro zone plate and film are both very inefficient (about 1% taken together) and they come AFTER the sample. Thus about one hundred times more damage is done to the sample than in an ideal experiment.

9. SCANNED IMAGE ZONE PLATE MICROSCOPY

In order to address the damage problem one would like to position the zone plate and its losses BEFORE the sample and use a nominally 100% efficient detector. These conditions are achieved by the scanning geometry illustrated in figure 5.[30] The zone plate focusses the beam to a diffraction limited spot, (i.e. a single mode beam is used) and the sample is then scanned through the spot in a raster pattern using high resolution piezoelectric tranducers. At each dwell position of the sample the x-ray count rate is recorded using a flow proportional counter which is close to 100% efficient in the soft x-ray region. Additional advantages of this scheme are the convenience with which the data can be stored and manipulated by the computer, the fact that the sample can be kept in atmospheric pressure air or helium and the natural way the arrangement lends itself to absorption microanalysis. Against these considerations is the requirement for an x-ray beam with full spatial coherence and the serial nature of the data taking. Both of these factors lead to long exposure times. The leading group in this field to date is based at the State University of New York at Stony Brook and the NSLS. The Stony Brook microscope presently makes pictures of 140x140 pixels with resolution 1200Å in about one hour using a bending magnet source on the Brookhaven VUV ring (see fig 6 for example).

10. SCANNED IMAGE REFLECTION MICROSCOPY

One of the difficulties leading to slow imaging using scanned image zone plate microscopy is the need for full spatial coherence. This problem can be addressed at least in principal by forming the x-ray focal spot using reflective optics instead of a zone plate. The idea would be to use a very fast optical system, say f1 for example. This could have a diffraction limited resolution of 1xλ=30Å. Enlarging the source pinhole diameter by a factor of ten then leads to a system with 300Å resolution and 100 times greater phase space acceptance than any diffraction limited system.

Various reflective optical systems have been proposed in the past. Those due to Kirkpatrick and Baez, and Wolter both use grazing angles of a few degrees and were originally intended to image the entire transilluminated sample in the manner of a lens. The use of these systems to create a focal spot only one pixel wide, i.e. to image with a negligibly small field angle, has the important advantage of eliminating almost all of the geometrical aberrations that would otherwise limit the resolution. The resolution will then be limited by fabrication tolerances so that the Kirkpatrick-Baez system with its spherical surfaces has a great advantage. It also has a rectangular aperture which is a better match to a synchrotron radiation beam than the annular aperture of the Wolter scheme. In the opinion of this author the use of the Kirkpatrick-Baez system to do scanned image microscopy (or microanalysis for that matter) has a breat deal to recommend it.[31] It would certainly give better efficiency than a present day zone plate. The challenge would be to equal the zone plate in the important matter of resolution.

The most ambitious form of scanned image reflection microscopy is based on the use of normal incidence optics. A double bounce Schwartzchild optical scheme[32] can be used with the optics made reflective in the soft x-ray region by the use of multilayer coatings (see fig 7). The latter also supply the function of a monochromator. Very fast systems (f10 or better) are possible but the barrier to good resolution is the need to fabricate the two spherical surfaces with extremely fine

tolerances. The situation is even worse than in the grazing incidence case because grazing incidence surfaces are more forgiving of surface imperfections than normal incidence ones by a factor of roughly $(\mathrm{Sin}\theta)^{-1}$ where θ is the grazing angle. The estimated figuring accuracy required for the spherical surfaces of a Schwartzchild x-ray "lens" is around 10Å for 300Å spatial resolution. This is probably possible if suitable measuring equipment can be obtained but existing capability is nearer to the 50Å level.[33]

11. SOFT X-RAY HOLOGRAPHY AND DIFFRACTION

The techniques described so far provide very little, if any, three dimensional information. However, as the resolution of the methods improve the two dimensional images of objects whose thickness is many times the transverse resolution will become more and more complicated and difficult to interpret. Now we know (see section 5) that the sample scatters a three dimensional wavefield which can, in principle, be detected (in both amplitude and phase) and backpropagated to yield information about the three dimensional structure of the sample. This process, even in principle, is subject to important limitations which are best understood by considering the Fourier space $\underline{K} \equiv (K_x, K_y, K_z)$ representation of the sample. It can be shown that from a given view direction we can only learn about the sample Fourier components which lie on the Ewald Sphere[37] in $\underline{K}$ space where $\underline{K}$ is the momentum transfer to the sample in the x-ray scattering process (see fig 8). If the wavefield is detected over only part of the 4π solid angle into which it is emitted then frequencies lying on only part of the Ewald Sphere will be probed. In other words an optical system, accepting a cone of half angle ϕ has transverse bandwidth limits given by

$$K_x^{Max}, K_y^{Max} = \frac{2\pi \mathrm{Sin}\phi}{\lambda}$$

and a corresponding maximum for K_z given by the condition that $(K_x^{Max}, K_y^{Max}, K_z^{Max})$ must lie on the Ewald sphere (see figure 8). If the wavefield is measured over the full 4π solid angle for enough different illumination directions then the image can be reconstructed with resolution $\lambda/2$. The algorithm by which the sample Fourier components

can be determined from measured values of the amplitude and phase of the scattered field is given by Wolf[34] for the case of the Born Approximation[16] (negligible depletion of the incident field by scattering or $\psi(\underline{r}') \simeq e^{ik_o z}$ in (3)).

Since very little experience has been gained even in the visible region, in reconstructing true three dimensional optical density distributions (as opposed to surfaces bounding an opaque object) it is difficult to say how many views will be needed to give useful biological information. It is desirable on damage grounds to keep the number small.

The problem of reconstructing an object from the measured scattered fields resulting from illumination in various directions is known as the "diffraction tomography" problem. It occurs in various fields of engineering, particularly, seismology, ultrasonics and radar and has an extensive literature.[35,36]

For the case of interest to us: scattered soft x-rays, the problem of measurement of the wave field is considerably more difficult than in the above cases. This is because the x-ray frequencies involved are far beyond the range of practical phase measuring detectors. Consequently, only intensity measurements will be available and in order to make progress it is necessary to find a method for obtaining the phases.

The solution of such phase retrieval problems has been a preoccupation of crystallographers[38] for many years and has received renewed attention recently from the viewpoints of electron microscopy[39], speckle interferometry,[40] radiometry[41] etc. Apart from the somewhat specialized crystallographic methods a typical approach is to make intensity measurements which, in spite of being noisy, contain as much redundancy as possible, e.g. measurements are made at several planes which are related to each other by the propagation operation or the Fourier inversion operation. The measured data are then supplemented by prior knowledge about the scattering density such as the shape of the region over which it has non-zero values (its "support"), its positivity etc. and an attempt is then made to calculate the phases from the intensity data. The calculations tend to be difficult and expensive and the results are open to complex questions of uniqueness. For soft x-ray

experiments they are still in the development stage. However, difficult as they are, they have one great advantage: they make the experiment easier and this is of critical importance. The recording and use of intensity-only soft x-ray data is known as "soft x-ray diffraction" and this approach is beginning to be applied successfully by D. Sayre and W. Yun.[42] See figure 9.

The alternative approach to obtaining the phases is to measure them. This can be done by beating the diffracted beams against a coherent reference wave. The resulting recording contains patterns of interference fringes which encode both amplitude and phase information and is therefore known as a "hologram". Roughly speaking this approach tries to avoid the difficulties of the phase calculation by making the experiment more difficult.

There is a considerable history of attempts to do holography using x-ray tubes going back to the early 1950's.[43] These experiments were never sufficiently successful to be applied to scientific investigations. They reached a peak with the work of Aoki et al[44] in the early 1970's and have since been abandoned. The chief reason for the failure of this approach was the poor coherence properties of the x-ray tube source. Now that sources with many orders of magnitude more coherent flux are available, the chances of doing successful x-ray holography at biologically interesting resolution levels is correspondingly increased. See figure 11. A series of experiments have recently been done by the present author and collaborators[43] using bending magnet radiation from the Brookhaven VUV ring. These have demonstrated a resolution of 1-2 μm for sparse, two dimensional, test objects using Gabor (in line) holography. Recording was on photographic film and reconstruction was by a helium cadmium laser (4416Å)(see figure 10). Improved resolution is expected in future experiments utilizing an undulator source (NSLS X1 in figure 11) and high resolution x-ray resist for recording. In this case reconstruction would best be done numerically. Future experiments using Fourier transform geometry are also anticipated.

ACKNOWLEDGEMENTS

The author wishes to acknowledge continuing valuable discussions on these matters with J. Kirz, D. Sayre and R. Feder.

REFERENCES

1. D. Parsons (ed), Conference on "Short Wavelength Microscopy" Ann. N.Y. Acad. Sci. 306(1978)
2. D. Parsons (ed), Conference on Ultra Soft X-ray Microscopy; its application to biological and physical sciences. Ann. N.Y. Acad. Sci, 342(1980)
3. G. Schmahl and D. Rudolph, "X-ray Microscopy" Proceedings of a conference at Gottingen, Springer Verlag, Berlin, 1984
4. J. Kirz and D. Sayre in "Synchrotron Radiation Research", Plenum, New York, 1980
5. J. Kirz and H. Rarback, Rev. Sci. Inst 56, 1(1985)
6. M. Howells, J. Kirz, D. Sayre and G. Schmahl, Physics Today, 38, 8, 22(1985)
7. V.E. Cosslett and W.C. Nixon, "X-ray Microscopy", Cambridge University Press, Cambridge, 1960
8. G.J. Burch, Nature, Lond. 54, 111(1896) and F. Ranwez, C.R. Acad. Sci, Paris, 122, 841(1896)
9. P. Kirkpatrick and A.V. Baez J. Opt. Soc. Am. 38, 766(1948)
10. H. Wolter Ann. Phys, 10, 94(1952)
11. See reference 7 section 11.13
12. There is a series of conferences entitled X-ray Optics and Microanalysis and similar titles which began in 1956 and has continued at 3 year intervals until the present. Originally these had valuable information about x-ray microscopy but this diminished to a low value by about 1970. The first five were at location (editor, publisher) as follows; 1956 Cambridge (V.E. Cosslett, A. Engstrome and H.H. Pattee Academic), 1959 Stockholm (A. Engstrom, V.E. Cosslett, H.H. Pattee, Elsevier) 1962 Stanford (H.H. Pattee, V.E. Cosslett and A. Engstrom, Academic), 1965 Orsay (R. Castaing, P. Deschamps, J. Philibert, Hermann), 1968 Tubingen (G. Mölenstedt, K.H. Gaukler, Springer Verlag).
13. See the discussion in lecture 1 of this series of 4 lectures and references therein. For the electron data see D. Sayre, J. Kirz, R. Feder, D.M. Kim and E. Spiller Ultramicroscopy 2, 339(1977)
14. In the water window region the fluorescent yield of K shell vacancies

is very low and the use of K edges for elemental identification must be based on absorption. There are, however, many other cases when fluorescence is valuable. For general discussions see W. Bambynek et al, Rev. Mod. Phys 44, 716(1972) and C. Sparks, loc. cit. ref.4.

15. D. Sayre et al, loc. cit. ref 13.
16. N.F. Mott and H.S.W, Massey, "The theory of atomic collisions" 2nd ed., Oxford, 1949 Equation (3) is derived in paragraph 4 of chap. VI
17. See for example E.F. Plechaty, D.E. Cullen and R.J. Howerton UCRL - 50400 - Vol 6, Rev 3, Lawrence Livermore Laboratory, 1981
18. J. Kirz, J. Opt. Soc. Am. 64, 301(1974)
19. M.R. Howells, J. Kirz and S. Krinsky, A beamline for experiments with coherent soft x-rays, Brookhaven report BNL 32519(1982)
20. D.T. Attwood, K.J. Kim, K. Halbach and M.R. Howells Lawrence Berkeley Lab report LBL 20569 SPIE Conference on Magnetic Undulators and Wigglers, Stanford, 1985
21. M. Born and E. Wolf "Principles of Optics", Pergamon, Oxford (1980)
22. J.W. Goodman, "Statistical Optics", Wiley, New York, 1985
23. D. Attwood, K. Halbach and K.J. Kim, Science, 228, 1265(June 14, 1985)
24. R.W. James, "The Optical Principles of the diffraction of x-rays", Ox Bow, Woodbridge, Ct, 1982. The wave physics of the refractive index are well treated in sections II2b, II3b and IV1c
25. See for example Feder et al Science, 227, 63(4 Jan, 1985), Sayre et al loc. cit. ref. 2, Cheng et al, Baldini et al and Feder and Mayne-Banton all in Proc. Annual Conf. of Electron Microscopy Society of America (1985)
26. E. Spiller and R. Feder in "X-ray Optics", H.J. Queisser (ed), Topics in Applied Physics, 22, Springer-Verlag, Berlin, 1977
27. J.C. Solem and G.C. Baldwin, Science, 218, 229(1982)
28. D. Rudolf et al loc. cit ref 3
29. B. Nieman, D. Rudolf and G. Schmahl, Nucl. Inst. Meth 208, 367(1983) and G. Schmahl et al loc. cit. ref. 3
30. H. Rarback, Ph.D. Thesis, State University of New York at Stony Brook, 1983 and Kenney et al Nucl. Inst. Meth. 222, 37(1984)
31. M.R. Howells and J. Hastings, Nucl. Inst. Meth. 208, 379(1983)

32. I. Lovas, W. Santy, E. Spiller, R. Tibbetts, J. Wilczynski Proc. SPIE 316, 90(1981)
33. E. Spiller private communication
34. E. Wolf, Opt. Comm. 1, 153(1969)
35. A.C. Kak in "Array Signal Processing" Prentice Hall, Englewood Cliffs, 1985
36. A.J. Devaney, in "Inverse Methods in Electromagnetic Imaging Part 2", W.M. Boerner (ed), Reidel, 1985
37. R.W. James loc. cit ref. 24, p.71
38. See for example A.J.C. Wilson, "Elements of X-ray Crystallography", Addison-Wesley, Reading, Mass, 1970
39. W.O. Saxton, "Computer Techniques for Image Processing in Electron Microscopy", Academic, New York, 1978
40. J.C. Dainty in "Laser Speckle and Related Phenomena", J.C. Dainty (ed), Springer-Verlag, Heidleberg, 1975
41. H.P. Baltes (ed) "Inverse Source problems", Topics in current physics, 9, Springer-Verlag, Berlin, 1978
42. D. Sayre, R.P. Haelbich, J. Kirz and W. Yun lot. cit. ref. 3 and W. Yun, J. Kirz and D. Sayre, Act. Cryst. A to be published
43. M.R. Howells, J. Kirz and M. Iarocci, submitted to J. Opt. Soc. Am. LBL reprint #LBL21364
44. J.C. Solem and G.F. Chaplin, Opt. Eng. 23, 193(1984)
45. P.C. Cheng, Ph.D. Thesis, Univ. of Illinois at Chicago, 1985 (Univ. Microfilm International #85-21917)

FIGURE CAPTIONS

Fig 1. Absorption length data for protein and water for imaging particles. Upper half of diagram refers to soft x-rays[44], lower half to electrons[13]

Fig 2. Notation for theoretical discussion

Fig 3. SEM-magnified x-ray contact images of Xenopus laevis (frog) muscle cell[45]. A: SEM-magnified x-ray contact image of an osmium-fixed Xenopus laevis muscle cell. Note the regularly spaced Z lines of the sarcomeres. Within the cell nucleus, superimposed myofibrils are evident (arrows). However, due to the viewing position, some of the sarcomeres (arrows) are not easily recognized in photo B. Note the high x-ray absorption of the nucleolus. C:K image. G: EM grid, Y: yolk granule. B: The same resist as shown in A, but viewed at a different angle. Between Z lines, three x-ray dense bands can be observed (short arrows). Note the images of the nucleolus (No) and nucleus are superimposed with myofibril's image. C: SEM-magnified x-ray contact image of osmium-fixed Xenopus laevis muscle cell. Note the high x-ray absorption of the yolk granule (Y). The resist has been developed for a relatively long period. The under exposed parts (e.g., the yolk granule (Y)) begin to show structures (arrows). However, these structures may only represent superimposed images of other cytoplasmic structures. N: nucleus, No: nucleolus, D: diffraction fringe. Reproduced by courtesy of P.C. Cheng and R. Feder

Fig 4. Optical layout of zone plate imaging microscopy as practiced by the Gottingen group

Fig 5. Overall layout of zone plate scanned image microscopy as practiced by the Stony Brook Group

Fig 6. Example of absorption microanalysis carried out using the Stony Brook microscope. (a) image of human bone sample taken on the high absorption side of the calcium L edge, (b) the same picture taken on the low absorption side of the Ca L edge. Blue indicates zero absorption (i.e. a hole) in both cases. (c) subtraction of (a)-(b) to give a calcium map. Blue now indicates highest calcium, black represents a hole. Reproduced by Courtesy of J. Kirz

Fig 7. Use of Schwartzchild objective coated with multilayer reflectors for scanned image reflection microscopy

Fig 8. Geometry of the Ewald sphere. For an optical system of acceptance half angle ϕ in real space, the spatial frequency bandwidths in the x and y direction are given by $K_x=K_y<2\pi Sin\phi/\lambda$. The values of K_z that correspond to these values of K_x and K_y are the ones that lie on the Ewald sphere with radius $2\pi/\lambda$. Thus for any experiment with a single view angle the K_x,K_y,K_z values that can be probed are those lying within the cap of the Ewald sphere passing through the origin as marked in the diagram.

Fig 9. (a) Visible light micrograph of diatom sample used for soft x-ray diffraction experiment (400x), (b) scanning electron micrograph of the same diatom showing structures with a periodicity of about 2000Å (c) soft x-ray diffraction pattern showing features corresponding to the 2000Å periodicity in 1st, 2nd and 3rd order.

Fig 10. General representation of Gabor in-line holography experiment. Hologram was recorded using synchrotron radiation (λ=32Å) and reconstructed using a helium cadmium laser (λ=4416Å)

Fig 11. Spectral brightness for several synchrotron radiation sources and conventional x-ray sources. The data for conventional x-ray tubes should be taken as rough estimates only, since brightness depends strongly on such parameters as operating voltage and take-off angle. The indicated two-order-of-magnitude ranges show the approximate variation that can be expected among stationary-anode tubes (lower end of range), rotating-anode tubes (middle), and rotating-anode tubes with microfocusing (upper end of range).

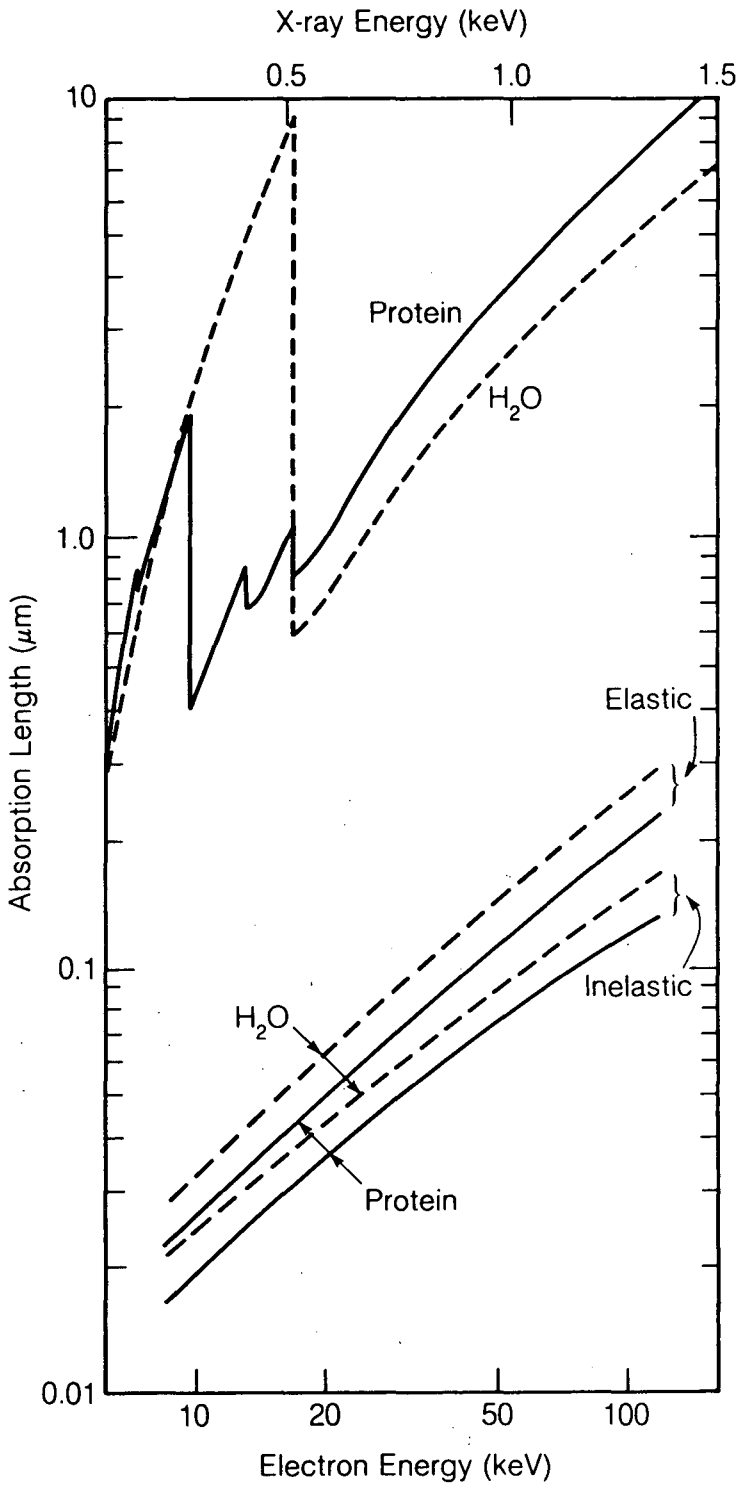

XBL 8411-5961

Fig. 1

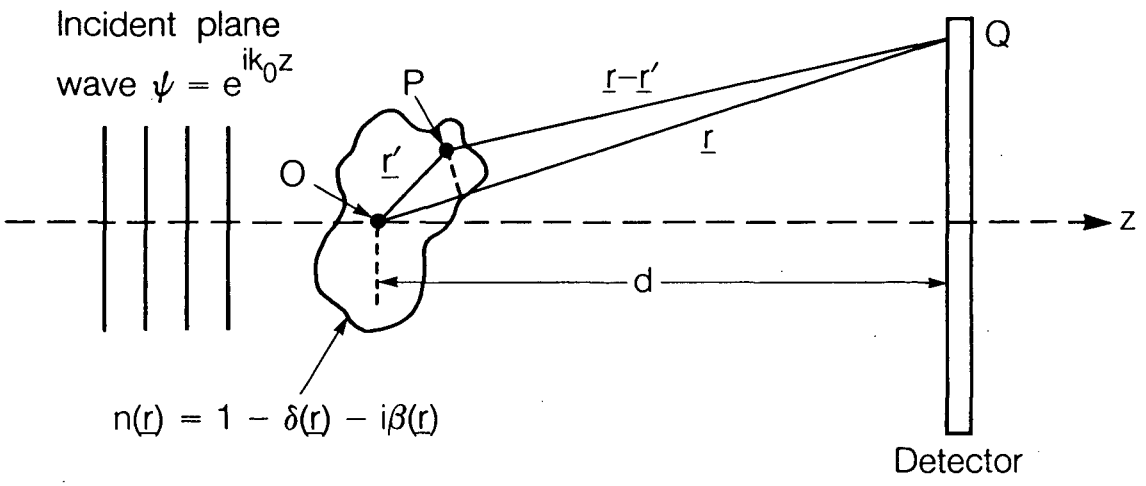

XBL 8411-5959A

Fig. 2

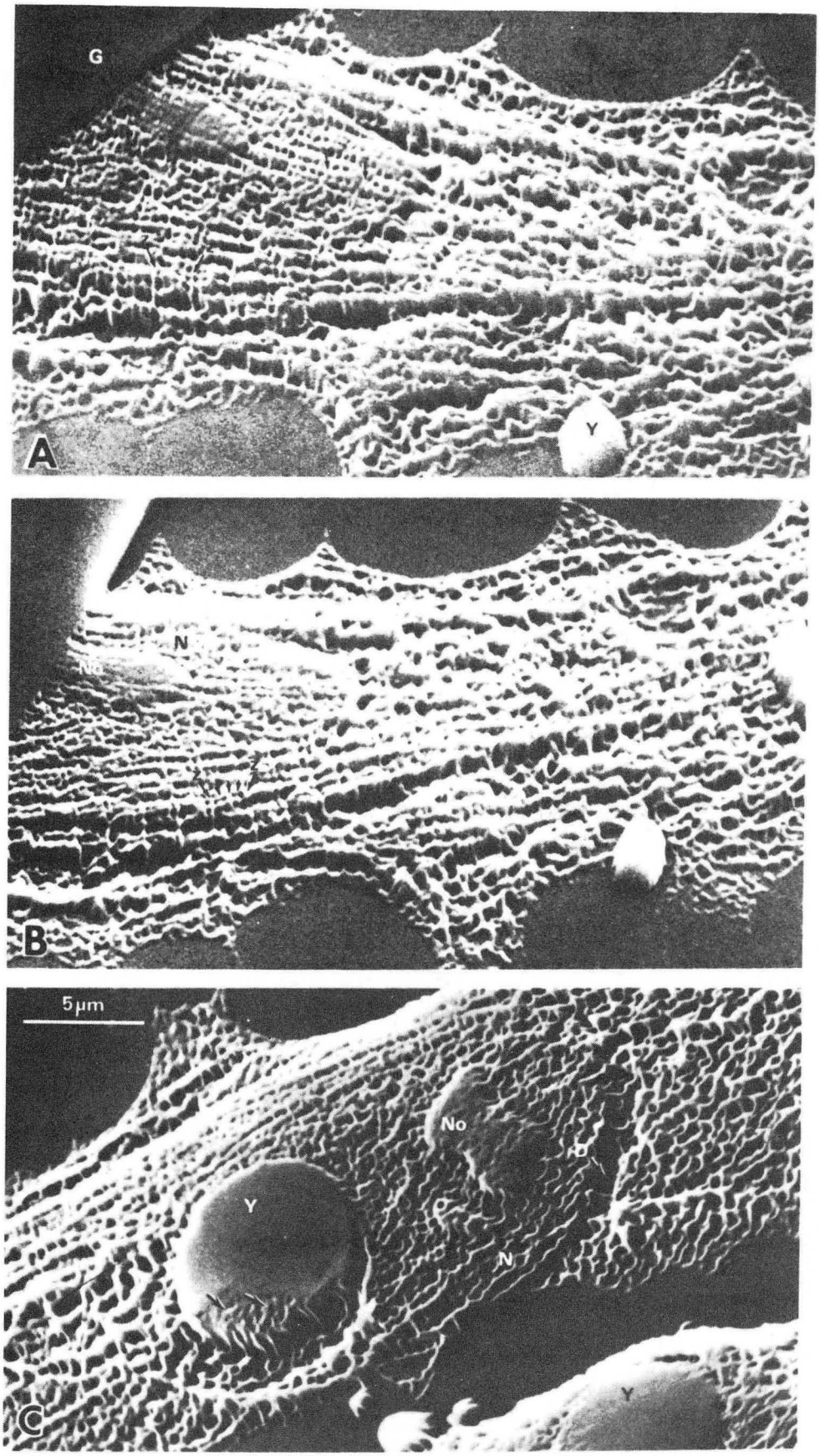

XBB 864-2616

Fig. 3

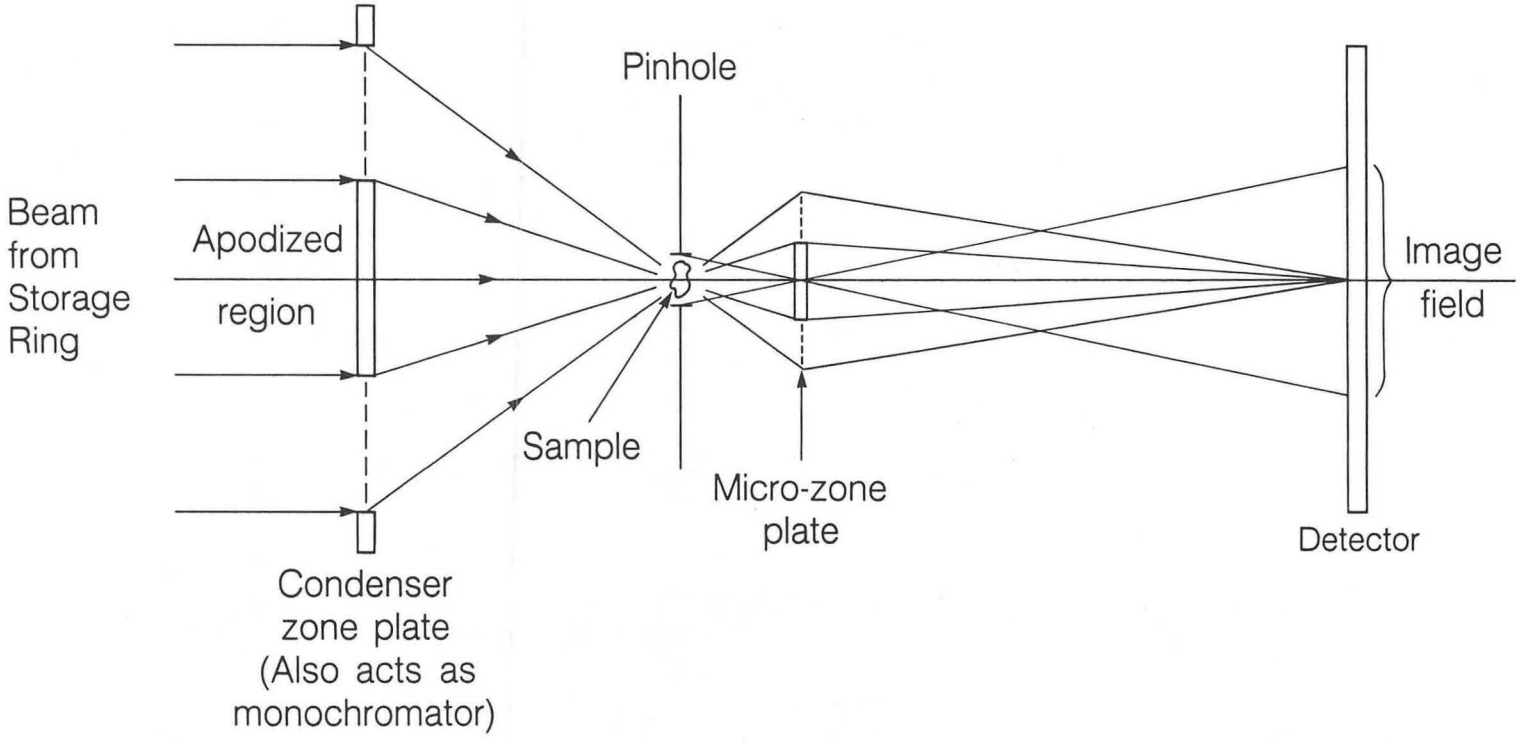
Beam
from
Storage
Ring
Apodized
region
Pinhole
Sample
Micro-zone
plate
Image
field
Detector
Condenser
zone plate
(Also acts as
monochromator)
XBL 863-9791

Fig. 4

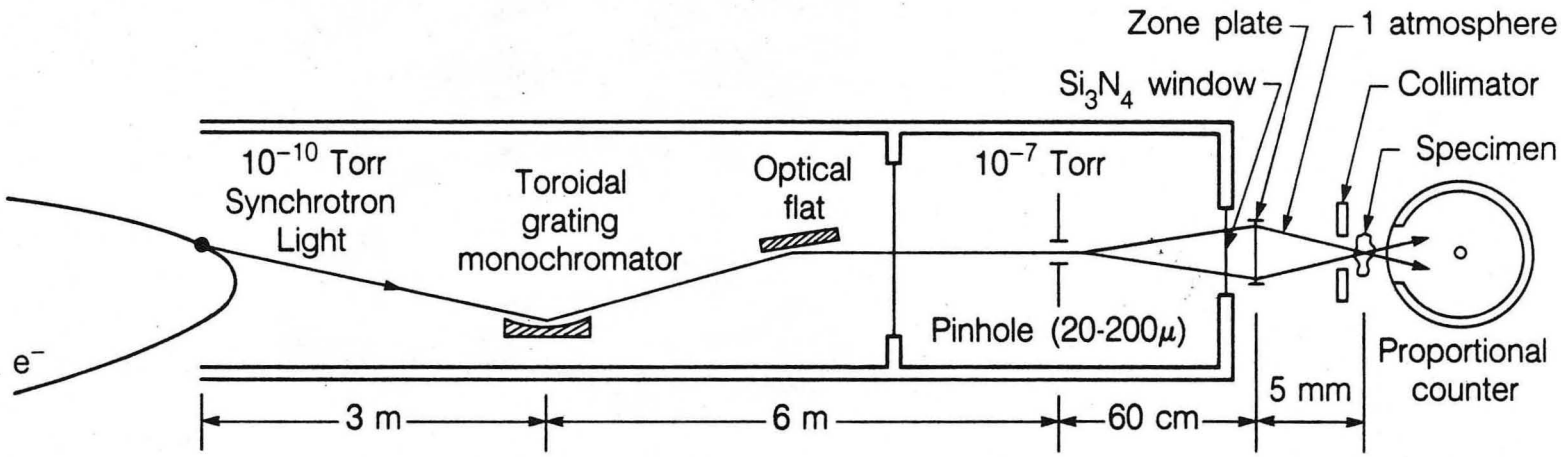
Zone plate
1 atmosphere
Si_3N_4 window
Collimator
Specimen
10^{-10} Torr
Synchrotron
Light
Toroidal
grating
monochromator
Optical
flat
10^{-7} Torr
Pinhole (20-200μ)
Proportional
counter
e^-
3 m
6 m
60 cm
5 mm
XBL 863-9789

Fig. 5

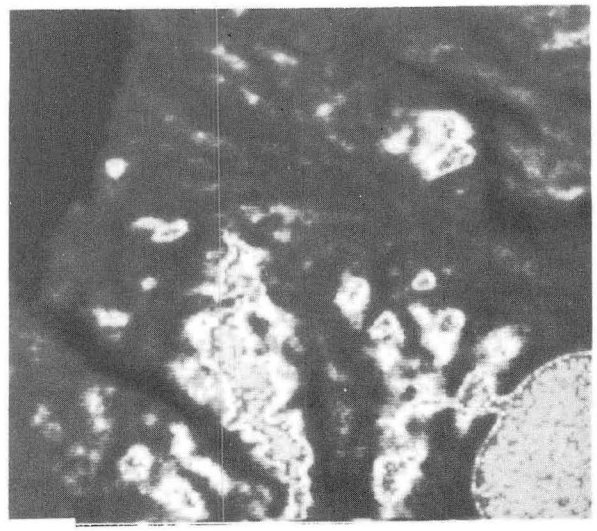

(a) 4 μm

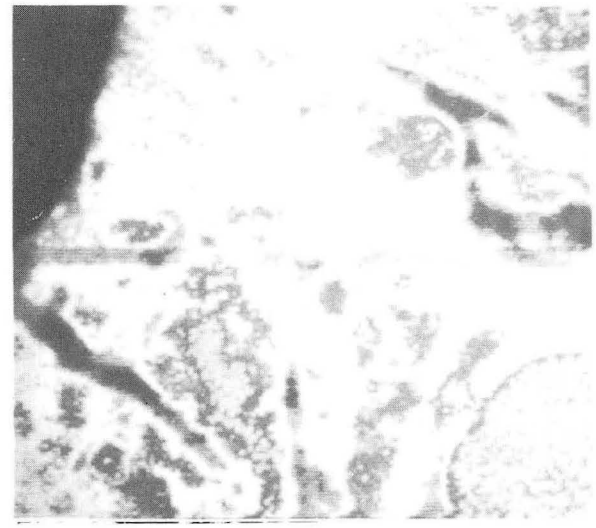

(b) 4 μm

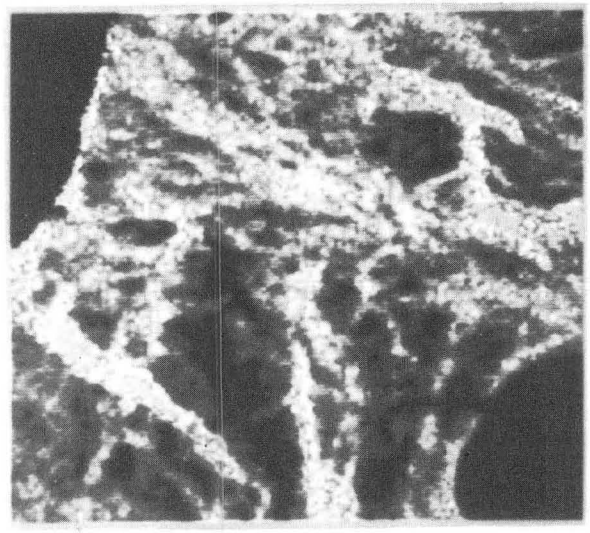

(c) 4 μm

CBB 864-2614

Fig. 6

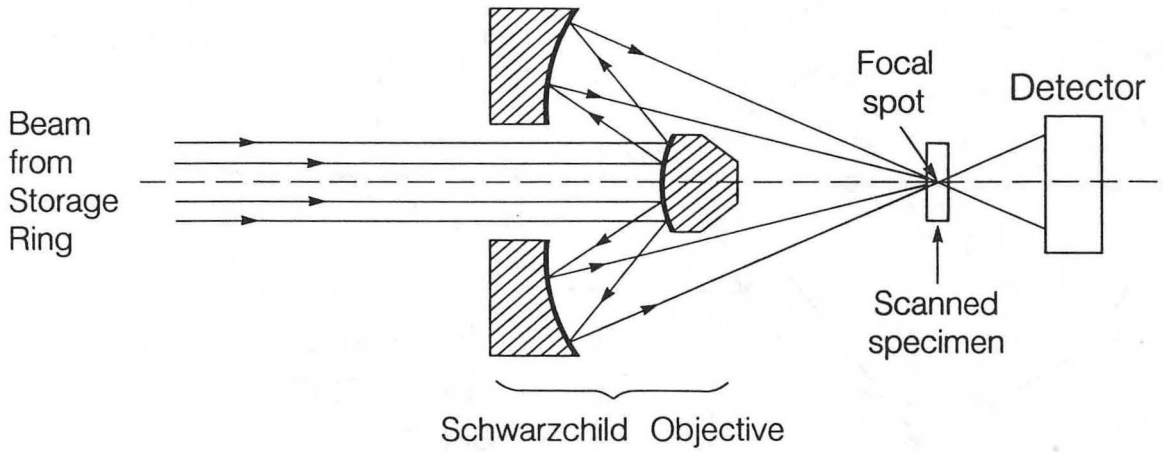

XBL 863-9790

Fig. 7

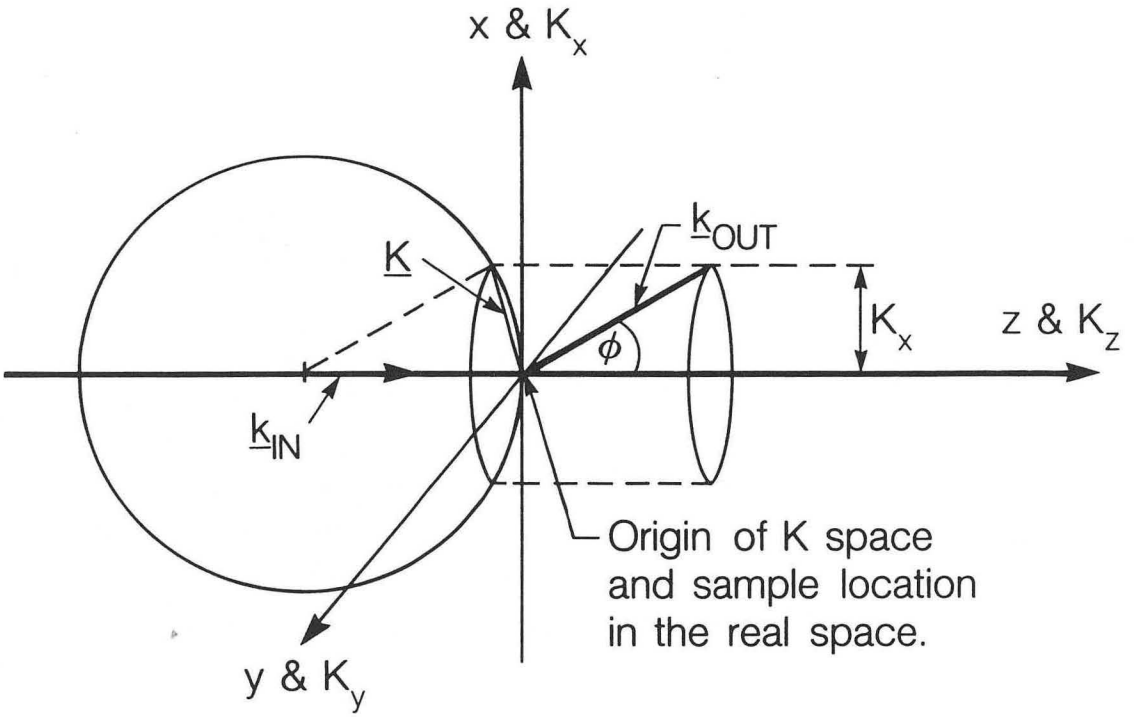

XBL 863-9788

Fig. 8

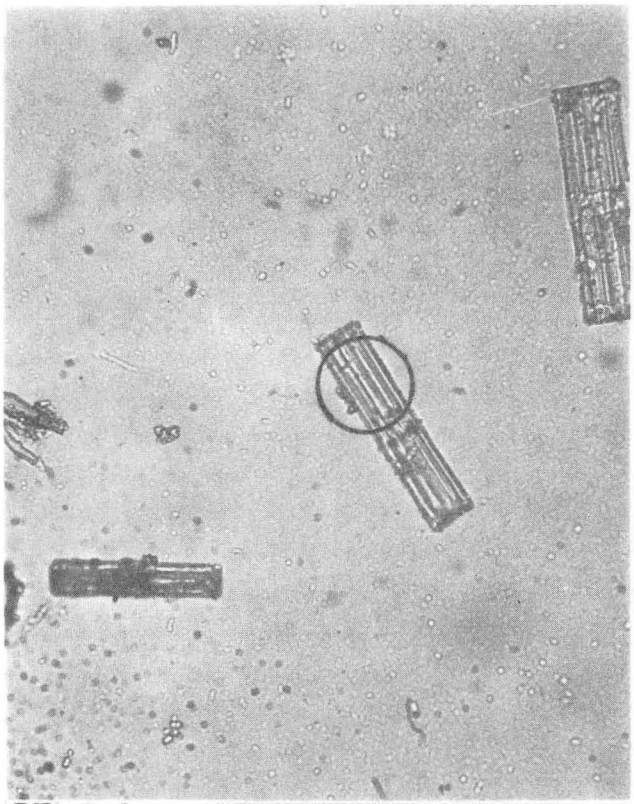

(a)

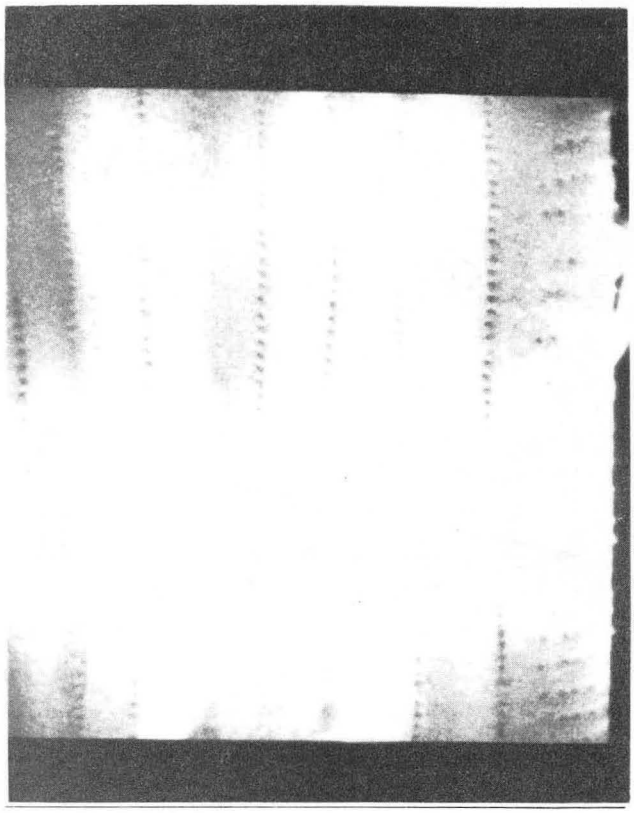

(b)

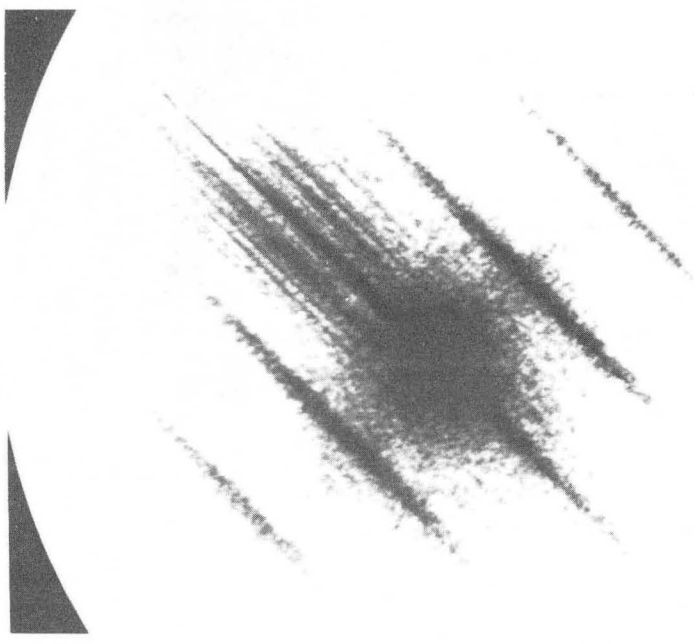

(c)

XBB 864-2617

Fig. 9

X-RAY HOLOGRAPHY

STEP ONE: Recording

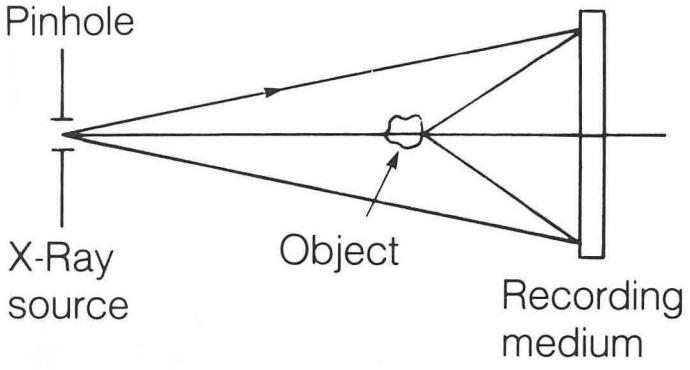

Hologram

STEP TWO: Reconstruction

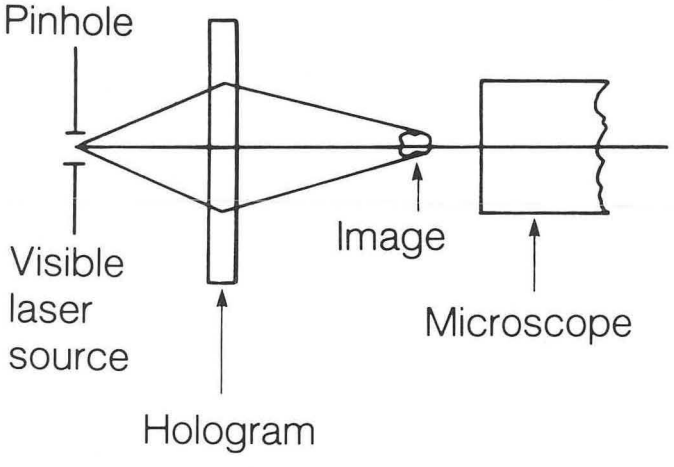

Holograms recorded at Brookhaven National Laboratory
By M.R. Howells* and M. Iarocci
*Now at Lawrence Berkeley Laboratory

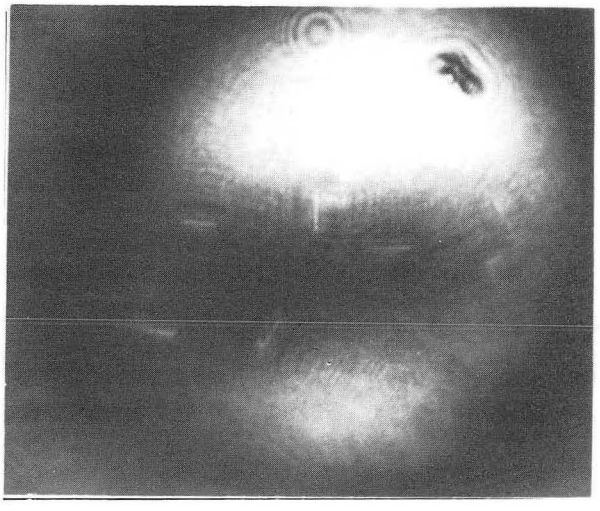

Reconstructed image
asbestos fibers
0.5–2.0 μm dia

XBB 854-2089A

Fig. 10

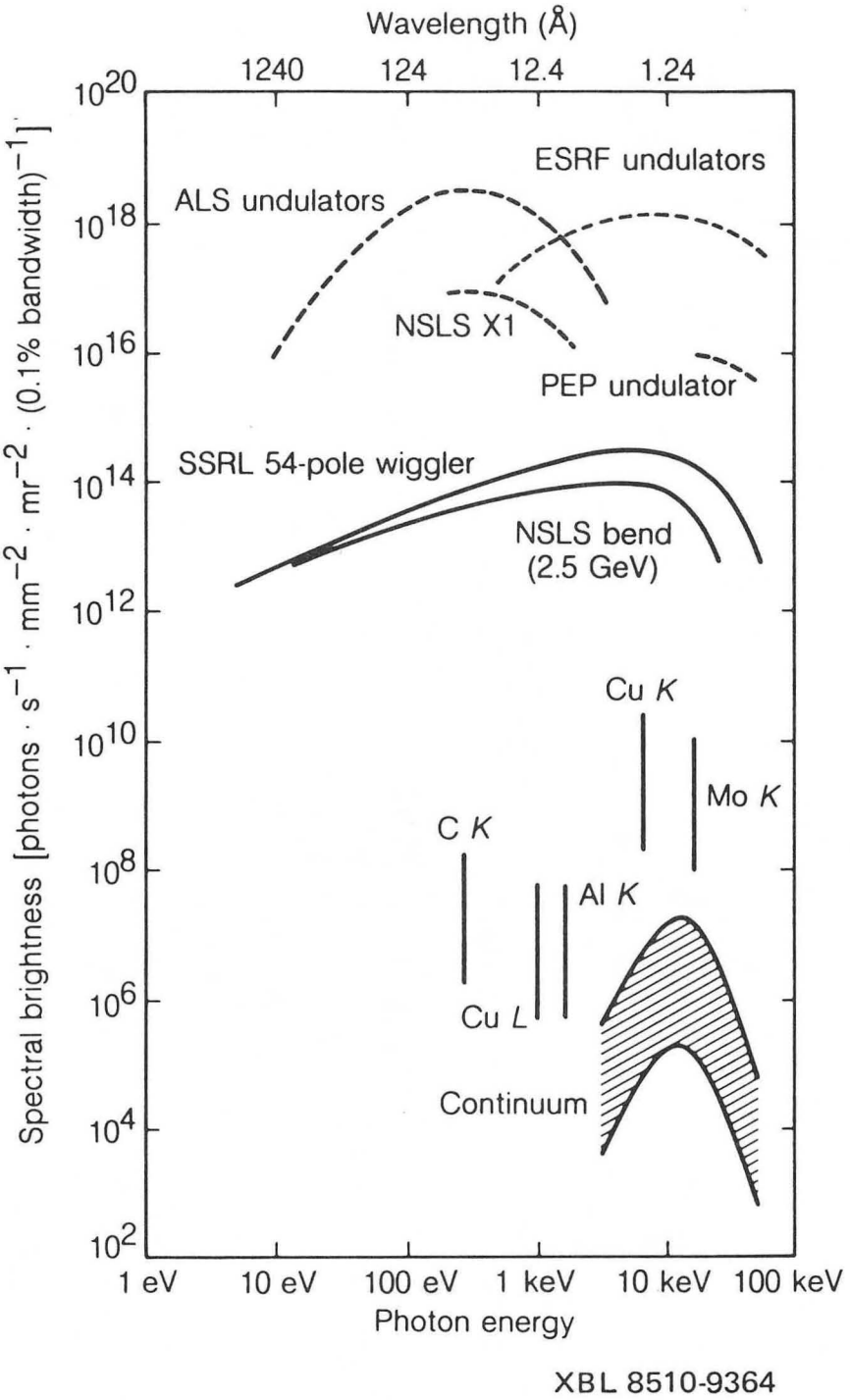
Wavelength (Å)
1240
124
12.4
1.24
10^{20}
10^{18}
10^{16}
10^{14}
10^{12}
10^{10}
10^{8}
10^{6}
10^{4}
10^{2}
Spectral brightness [photons · s^{-1} · mm^{-2} · mr^{-2} · (0.1% bandwidth)$^{-1}$]
ESRF undulators
ALS undulators
NSLS X1
PEP undulator
SSRL 54-pole wiggler
NSLS bend
(2.5 GeV)
Cu K
Mo K
C K
Al K
Cu L
Continuum
1 eV
10 eV
100 eV
1 keV
10 keV
100 keV
Photon energy
XBL 8510-9364

Fig. 11

This report was done with support from the Department of Energy. Any conclusions or opinions expressed in this report represent solely those of the author(s) and not necessarily those of The Regents of the University of California, the Lawrence Berkeley Laboratory or the Department of Energy.

Reference to a company or product name does not imply approval or recommendation of the product by the University of California or the U.S. Department of Energy to the exclusion of others that may be suitable.

LAWRENCE BERKELEY LABORATORY
TECHNICAL INFORMATION DEPARTMENT
UNIVERSITY OF CALIFORNIA
BERKELEY, CALIFORNIA 94720